UCID- 16707

LAWRENCE LIVERMORE LABORATORY
University of California/Livermore, California

PROPERTIES OF PARTICLE ORBITS IN AN AVERAGE-MINIMUM |B| MIRROR CONFIGURATION

R. P. Freis and R. W. Moir

February 1975

Prepared for U.S. Atomic Energy Commission under contract no. W-7405-Eng-48

PROPERTIES OF PARTICLE ORBITS IN AN AVERAGE-MINIMUM |B| MIRROR CONFIGURATION

R. P. Freis and R. W. Moir

Lawrence Livermore Laboratory, University of California

Livermore, California

February 1975

ABSTRACT

Calculations are presented of drift surfaces, particle orbits and J invariants ($J = \oint v_{\parallel} ds$) for a particular mirror configuration. These quantities are interesting because the particles with small $\mu(\mu = mv_{\perp}^2/2B)$ have drift surfaces which are not single valued and have J quantities which to lowest order are not invariant and in fact oscillate. The class of mirror confinement configuration we treat is known as average-minimum |B| in which the field lines are curved away from the plasma in places and towards it in others, but on the average are curved away. This particular configuration is of interest because it would be technologically much easier to build than a baseball or Yin-Yang configuration.

1. INTRODUCTION

This note is motivated by recent discussions about the existence and/or necessity of drift surfaces and J invariance in various mirror configurations. We present here the calculated orbits, drift surfaces, drift velocities and J invariants for a particular configuration. These quantities we think have interest in the above context because the particles with small $\mu(= mv_\perp^2/2B)$ have drift surfaces which are not single valued and have J quantities which to lowest order ($= \oint v_\parallel ds$) are not invariant and oscillate. This work is part of a forthcoming more comprehensive discussion on the equilibrium and stability properties of an average-minimum B mirror configuration. The class of mirror confinement configurations known as average-minimum $|B|$ is one in which the field lines are curved away from the plasma in places and towards it in others, but on the average they are curved away, and an example is shown in Fig. 1. The good curvature is produced by baseball coil (it could have been a Yin-Yang Coil or Ioffe bars) and the mirrors are produced by elliptical coils. Due to simple geometry, elliptical coils are technologically much easier to build than a baseball coil, particularly for mirror ratios greater than two. The connecting region is where the bad curvature occurs and could lead to low frequency flute instability

2. MAGNETIC DESIGN

The conductor configuration used for orbit calculations has the baseball coil represented by a single line current and elliptical mirror coils (actually they are rectangular) represented by 11 single line current at each end (Fig. 1). The current strengths are adjusted to give a central field of ~20kG and a maximum field of ~80kG at the mirrors in the elliptical coil region. A profile of $|B|$ as a function of z for r = 0 (dotted curve labeled on axis-"simplified", Fig. 2) shows secondary mirrors at z = $\pm$ 70cm. This may be an undesirable feature due to local trapping of some special orbits, but was not important for the orbits we studied, although it may have introduced extra nonadiabatic effects.

This conductor configuration was kept simple in order to reduce the time for computing orbits, however, a more complete and detailed conductor design was calculated in which the baseball coil was represented by 25 line current sources and two extra mirror coils were inserted near the baseball coil at each end (Fig. 3).

Some $|B|$ surfaces and field lines are shown in Fig 3. Note the field lines have good and bad curvature. This had the beneficial effect of eliminating the secondary mirrors near the axis of the machine (Fig. 2, solid curve labeled on axis-"improved"). This design did not eliminate secondary mirrors along all field lines (Fig. 2, dashed curve labeled outer line-improved) but this could probably be achieved with further refinements.

3. PARTICLE ORBITS, ADIABATIC LIMITS

The orbits were calculated using the guiding center model [3] and included only the vacuum B fields. The effects of the diamagnetism of the plasma is to reduce the magnetic field approximately by the factor $\sqrt{1 - B}$ which probably will not change our results significantly for $\beta \lesssim 1/2$. This model assumes the magnetic moment μ remains constant, however, if the orbit passes through regions in which the field changes more 20% in a gyro period, the particle is a called nonadiabatic. In addition, J is not assumed constant and is calculated for each transit from the integral $J = \oint v_{\parallel}\, d\ell$.

Some orbits were also calculated using the more time consuming particle equations of motion [4], which do not assume a constant μ and therefore can be used as a validity check of the guiding center calculations.

A group of deuterium ions was started near the center at z_0=7.96,θ_0=90°, and the initial r_0, μ and W (energy) were varied. At each subsequent crossing of the plane $z=z_p$ the time and position were saved and used to determine the drift surface and velocity v_T tangential to the surface for each particle.

Briefly stated, the results show that mirror trapped particles with small r_0 are contained and those with large r_0 hit the walls. Also, those particles with small μ, which therefore penetrate further down the z axis and experience fields with bad curvature, have the most unfavorable v_T .

With respect to varying r_0, it was found that low energy particles (W < 20 keV) with r_0=5, were adiabatically contained, whereas those with r_0=7 were not. To be more precise, the latter particles were found to go through nonadiabatic regions, which invalidates their subsequent calculated escape. To correctly determine these orbits requires solving the equations of motion for the particles rather than for the guiding centers. Such calculations do verify the nonadiabatic loss and in fact, predict [5] non-adiabatic loss for particles which in the guiding center calculations appeared to be confined in spite of passing through nonadiabatic regions. On the other hand, particles which appear adiabatically trapped in the guiding center calculation give the same results with the more exact calculations. In the light of these results we make the conservative rule of thumb that any guiding center orbits that pass through nonadiabatic regions will eventually be lost.

Using the above rule we find that for W > 20 keV. particles are non-adiabatically lost for r_0=5. This also depends upon μ as well as W. For convenience, μ is sometimes related to the initial condition paramenter

$u = v_\parallel/V$ by the equation.

$$u = (1 - \frac{B_0\mu}{W})^{1/2} \quad , \qquad 3.1$$

Where B_0 is the magnetic field at the initial position, $v_\parallel$ is the initial parallel velocity, and $\mu = 1/2\ m\ v_\perp^2/B$. Also, u is related to R_m, the mirror ratio of the particle by the equation

$$R_m = (1 - u^2)^{-1}, \qquad 3.2$$

recalling that $R_m \leq 4$ holds for the fields under consideration. In terms of the parameters W and R_m, particles with initial position r_o=5 that are adiabatically contained have a rapidly decreasing maximum R_m in the energy range 20 keV<W < 40 keV, as seen in Fig. 4 . We expect that for r_o<5 a similar bahavior would be found, with perhaps a slight increase in the corresponding energies.

To maintain our conservative bias, we regard 20 keV as the upper limit for adiabatically contained particles.

This limit is due to the steep field gradiants in the region between the baseball coil and the mirror coils (Fig. 2). For a 40 kG field the cyclotron period τ_c is 3.28 x 10^{-8} sec for D^+, during which time a 40 keV deuteron travels 6.4 cm. If the field increases by more than 20% over this distance, the adiabatic limit will be violated and this occurs in our simple configuration. For our improved configuration th slope has been reduced in the region near the z axis but is not much changed for the outer field lines (Fig. 2).

4. DRIFT SURFACES

A typical cross section of a drift surface in the plane z_p=o is illustrated in Fig. 5 (in which W=1.5 keV). The most prominent feature of this cross section is that it is composed of two closed curves which cross each other at θ=0°, 90°, 180° and 270°. This result is similar to earlier calculations of Siambis and Trivelpiece[6], where they also found the surfaces coming together near those field lines that have no torsion, as is true in our case for the field lines at 0°, 90°, 180°, and 270°. A particle alternates between one surface and the other on consecutive bounces, and each surface can be associated with the sign of v_z (some of the consecutive data points in Fig. 4 are numbered to illustrate this).

This is due to the average drift of the guiding center away from a field line over one bounce and in toroidal geometry results in banana orbits for trapped particles.[7] Morozov and Solov'ev show[8] that for time independent fields and $\underline{B}\cdot\nabla\times\underline{B}=0$, the drift equation has trajectories which coincide with a field B^* defined by

$$\underline{A}^* = \underline{A} + \frac{mc\, v_\parallel}{eB}\ \underline{B}$$

where $\underline{A}^*$ is the magnetic vector potential ($B^* = \nabla\times A^*$). For our purposes we note that the sign of the second term depends on the sign of $v_\parallel$ and this can lead to double valued trajectory surfaces, which is consistent with our calculated results.

The maximum radial distance ℓ between surfaces increases with increasing W (compare Fig. 6 in which w=9 keV with Fig. 5) and decreases with increasing μ (compare Fig. 7 with Fig. 6) or equivalently, decreasing J. Note that in comparing orbits of different energies, we consider particles with the same effective mirror ratio R_m(=$W/B_o\mu$) where B_o is the magnetic field at the initial position. In comparing particles of the same energy, Fig. 6 is almost at the limit of mirror containment (R_m=3.90) whereas Fig. 7 is for a particle confined to the central region (R_m=1.04). In the limiting cases, the ratio of ℓ/ρ_o (ρ_o is the larmor radius at the initial position) is 14 for both W=1.5 keV and W=9 KeV, that is, ℓ is proportional to ρ_o for the two cases. In the latter case ℓ is around half the maximum radius of the drift surface. ℓ is a measure of the radial distance over which the plasma communicates with itself in one bounce time and as such, is similar to the mixing length discussed by Fowler[9].

It should be noted that ℓ/ρ_o falls off quickly with decreasing u, and for example at u=.6, for both 1.5keV and 100keV, $\ell\ \rho_o \sim 1$. (Recall that in the limiting case u=.86) In other words, those particles with large ℓ are also the ones easiest to scatter into the loss cone.

The shape of the drift surfaces changes at different z_p planes. For example at z_p=8 (Fig. 8) the same surface as seen in Fig. 5 is reduced by 6 cm in width along y axis and increased by 6 cm in width along the x axis. These changes are consistent with the B field geometry.

We note that $|B|$ is almost constant in the initial z plane over the region of the surfaces. To the degree that this is true, the dependence of the drift surface upon the initial position of the particle is removed and starting the particle at any point on the surface would generate the same surface.

5. ADIABATIC INVARIANT

The quantity $I = \int_{\ell-}^{\ell+} v_\parallel \, d\ell$, where $\ell-$ and $\ell+$ are the orbit turning points, is found to vary from bounce to bounce for a given orbit. A typical plot of I vs n (bounce number) is shown in Fig. 9 for the case W=1.5 keV which corresponds to the drift surface of Fig. 5. Each n can be related to its position on the drift surface and this correlates the position of maximum and minimum radial separation between surfaces with the maximum and minimum variation of I. Odd and even points are connected separately (Fig. 9) to show the bahavior of I over each surface. The pointwise sum of the two curves would give a curve with $\Delta I \sim o$. The quantity $J = \oint v_\parallel \, d\ell$ is equal to the sum of 2 consecutive I's and departs from being constant as v_T increases, which is consistent with the theoretical ordering that $\omega_D/\omega_B \ll 1$, where ω_D is the drift frequency and ω_D is the bounce frequency (Note the point wise sum of the two curves corresponds to J for v_T=o). The solid curve in Fig. 9 showing J (actually J/2 for ease of plotting) vs. n gives a maximum $\Delta J/J$ of 0.009. For the case W=9 keV, maximum $\Delta J/J$=0.04.

As has been shown by Hastie, Taylor and Haas[10] the longitudinal invariant can be put in the form $J = J_o + \frac{m}{c} J$. Where $J_o = \oint v_\parallel \, ds$ and the principal part of $J_1 = -\sigma \int_{s_0}^{s} \frac{ds}{q} \chi_D \cdot \nabla J_o$. Here s is the distance along a field line from a turning point s_o χ_D is the guiding center drift velocity, $q=|v_\parallel|$ and σ is either $\pm$ 1, depending on the direction being parallel or antiparallel to the direction of B. The main point here is that our numerical results are consistent with this form since our calculation of J neglects J_1 and our resultant ΔJ is consistent with the form of J_1.

6. TANGENTIAL DRIFT VELOCITY v_T.

As was already stated, v_T is determined from the time and position of consecutive crossings of the plane $z = z_p$. This guarantees that each v_T is the average drift velocity over a bounce path. As in the previous section, separating odd and even crossings can generate separate v_T for each of the two drift surfaces (in which case v_T is an average over 2 bounces). v_T is found to vary over a surface and a typical case (for W=9 keV, R_m=3.9) is illustrated in which v_T is plotted as a function of its angular position θ along one of the surfaces (Fig. 10) for z_p=0. We note that the maximum variation in v_T is ∿ 35% peak to peak and the peaks occurs near the regions θ = 45, 135, 225, 305. A very similar curve displaced by 90° can be plotted for the other surface, as illustrated in Fig. 10 by x's, which are v_T points from the other surface plotted at θ-90° from their actual position. As expected, at different z_p planes v_T differs. The main effect as one moves away from the mid plane z_p=o is for the variation of v_T over a surface to increase, with the general shape of the curves staying similar. For our purposes we shall use the maximum v_T in the plane z_p=o when comparing different cases.

As we vary μ, keeping all other initial conditions fixed, we find for large μ (small u) v_T is fairly constant, and in the stable direction ($+v_T$) with respect to low frenquency flute modes. At some critical μ, v_T changes sign and for smaller μ (larger u) v_T is in the unstable direction with respect to fluting. This is as expected because large μ orbits are confined to the central region where the field has good curvature and small μ orbits can pentrate closer to mirrors, where there are regions of bad curvature. For the case W=1.5 keV we plot v_T vs, u for r_0=3 and 5 (Fig. 11). Note the similarity of both curves, particularly where they cross the axis v_T=o. Curves of similar shape are generated over the energy range of interest and in fact at W-100 keV the critical u value ($u=u_c$) at which v_T=o is still the same. Naturally the magnitude of v_T increases with increasing W and to a good approximation increases proportionally to W as expected.

REFERENCES

1. C. C. Damm, et al. (1966) UCRL-50002-66-1 P. 26
2. R. W. Moir, R. F. Post (1969) Nuclear Fusion 9 253
3. W. A. Perkins, D. Fuss "Mafco 11 - A Code for Calculating a Guiding Center Trajectory of a Particle in Magnetic and Electric Fields" UCRL-50438
4. J. H. Foote, et al (1964) UCRL-50002-66-1. P. 32
5. J. H. Foote, "Nonadiabatic Energy Limit versus Mirror Ratio in Magnetic Well Geometry" Plasma Physics Vol. 14, P. 543 1972
6. J. G. Siambis, W. A. Trivelpiece "Adiabatic Containment of Charged Particles in Combined Mirror - Multipole Cusp Magnetic Fields" Phy. of Fluids Vol. 8, No. 11 P. 2047 1965
7. B. B. Kadomtsev, O. P. Pogutse "Turbulence in Toroidal Systems" Reviews of Plasma Physics Vol. 5 (See P. 261 - 265)
8. A. I. Morozov, L. S. Solov'ev "Motion of Charged Particles in Magnetic Fields" Reviews of Plasma Physics Vol. 2 (See P. 228 - 229)
9. T. K. Fowler "Charge Exchange at the Surface of Mirror-Confined Plasmas" UCID 16264 (1973)
10. R. J. Hastie, J. B. Taylor and F. A. Haas, Annals of Physics, 41 302 (1967)

FIGURE CAPTIONS

Fig. 1 Average minimum |B| coil configuration

Fig. 2 Magnetic field strength on axis and on an outer field line (Dotted line - simplified configuration, Solid line - improved design)

Fig. 3 Field lines and |B| contours

Fig. 4 Maximum RM (Particle mirror ratio) for adiabatic confinement vs. W (particle energy)

Fig. 5 Guiding center drift surface in the plane z=o for particles with RM=3.97, W=1.5keV, ℓ/ρ = 14

Fig. 6 Guiding center drift surface in the plane z=o for particles with RM=3.90. W=9keV, ℓ/ρ = 14

Fig. 7 Guiding center drift surface in the plane z=o for particles with RM=1.04, W=9keV

Fig. 8 Guiding center drift surface in the plane z=8 cm. for particles with RM=3.97, W=1.5keV

Fig. 9 I $(=\int_{-\ell}^{\ell} v_{\parallel}\, d\ell)$ and J $(=(I_n + I_{n+1})/2)$ vs. n (bounce number) for particles with RM=3.97, W=1.5keV

Fig. 10 v_T (tangential drift velocity) vs. θ (angular position on drift surface) for particles with RM=3.90, W=9keV

Fig. 11 v_T (tangential drift velocity) vs. u $(= v_{\parallel}/v)$ for particles with W=1.5keV, Ro=5 and Ro=3 (Ro = initial radial position of particle)

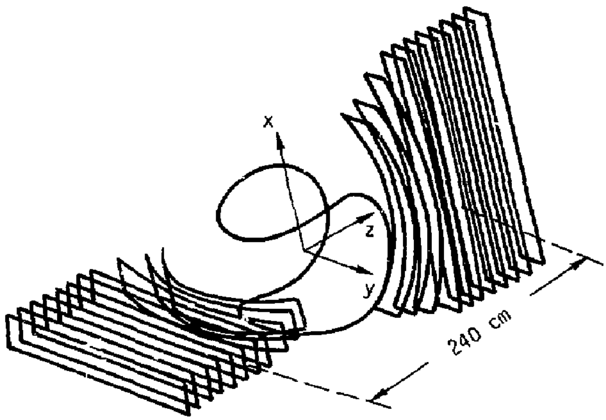
x
z
y
240 cm

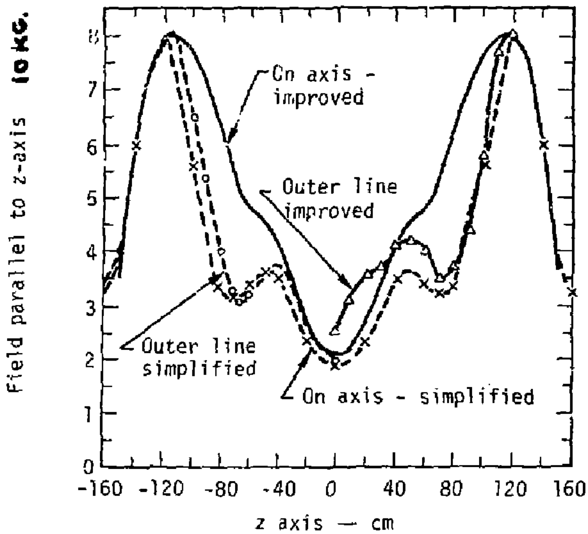
Field parallel to z-axis 10 KG.
On axis - improved
Outer line improved
Outer line simplified
On axis - simplified
z axis — cm
0
1
2
3
4
5
6
7
-160
-120
-80
-40
0
40
80
120
160

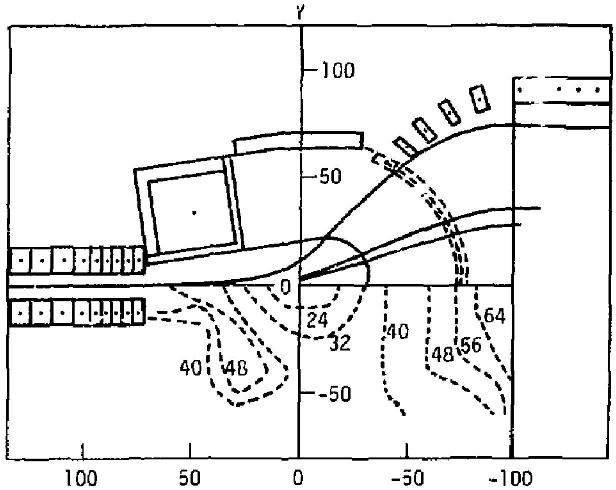
Y
100
50
0
24
32
40
48
40
48
56
64
-50
100
50
0
-50
-100

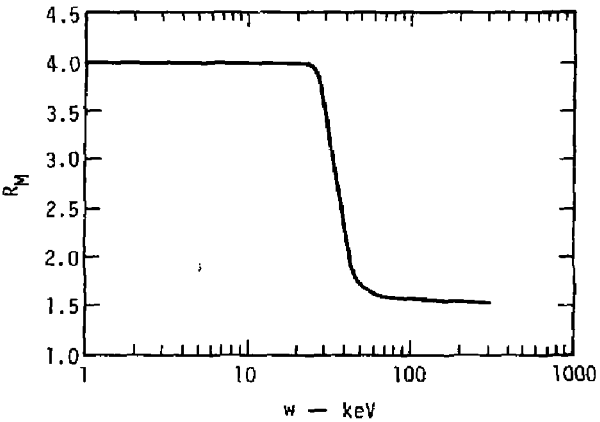
4.5
4.0
3.5
3.0
2.5
2.0
1.5
1.0
R_M
1
10
100
1000
w — keV

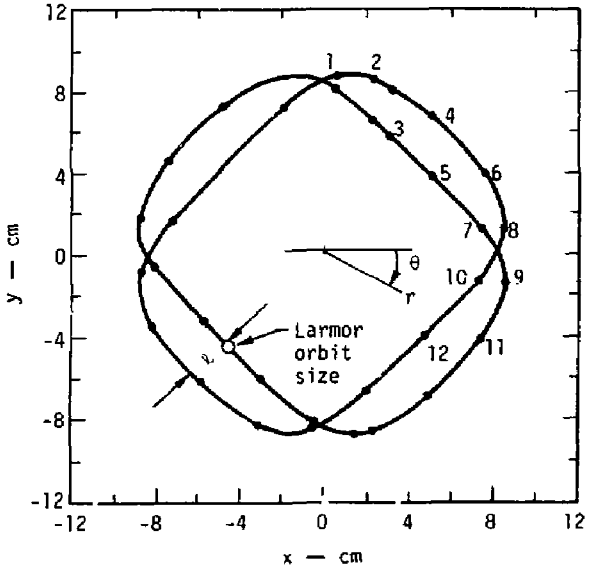

12
8
4
0
-4
-8
-12
-12
-8
-4
0
4
8
12
y — cm
x — cm
1
2
3
4
5
6
7
8
9
10
11
12
θ
r
Larmor
orbit
size

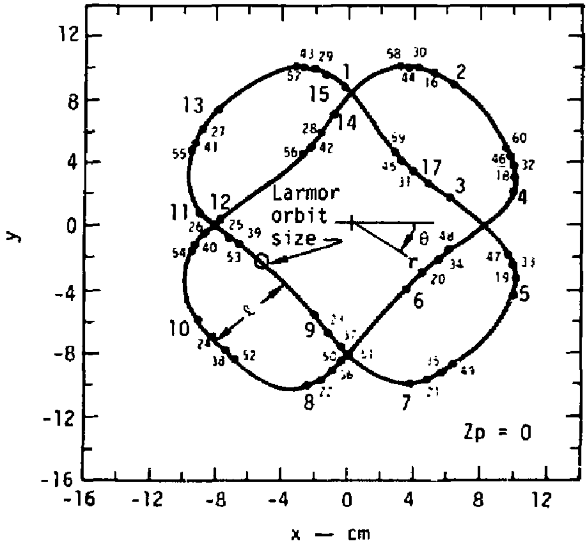
Larmor
orbit
size
θ
r
Zp = 0
y
x — cm
12
8
4
0
-4
-8
-12
-16
-16
-12
-8
-4
0
4
8
12

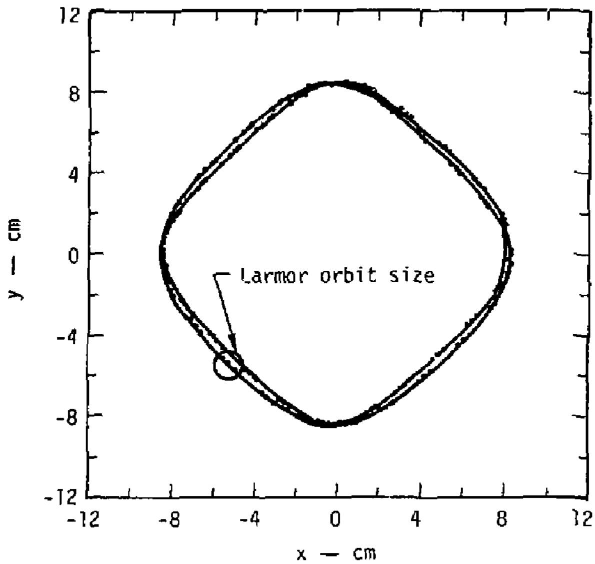
Larmor orbit size
12
8
4
0
-4
-8
-12
-12
-8
-4
0
4
8
12
y — cm
x — cm

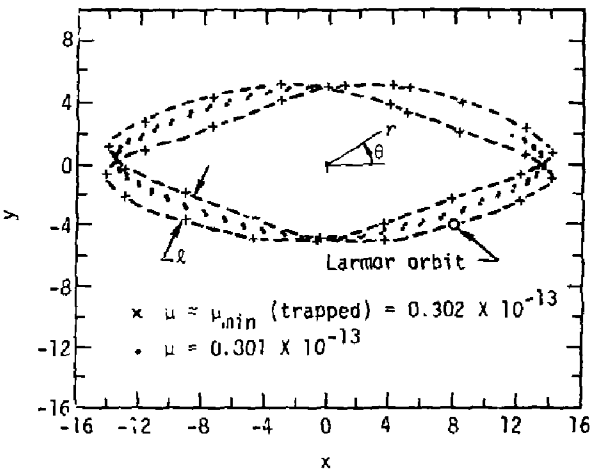

y
x
8
4
0
-4
-8
-12
-16
-16
-12
-8
-4
0
4
8
12
16
r
θ
ℓ
Larmor orbit
× μ = μ min (trapped) = 0.302 X 10-13
• μ = 0.301 X 10-13

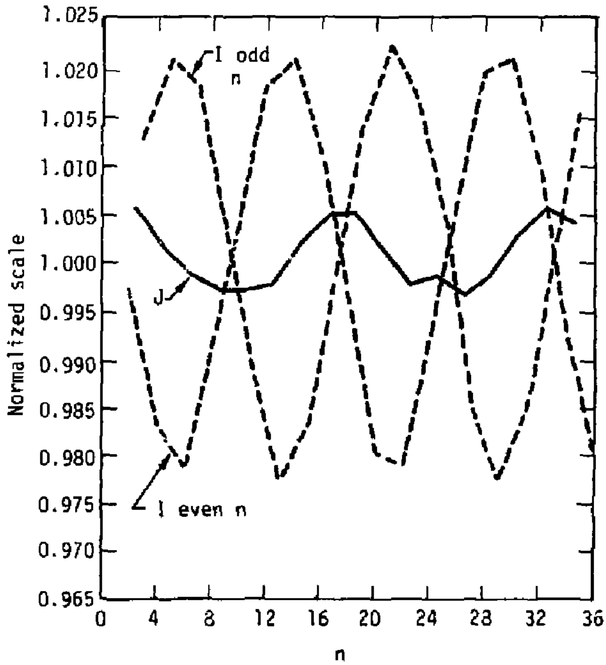
1.025
1.020
1.015
1.010
1.005
1.000
0.995
0.990
0.985
0.980
0.975
0.970
0.965
Normalized scale
I odd n
J
I even n
0
4
8
12
16
20
24
28
32
36
n

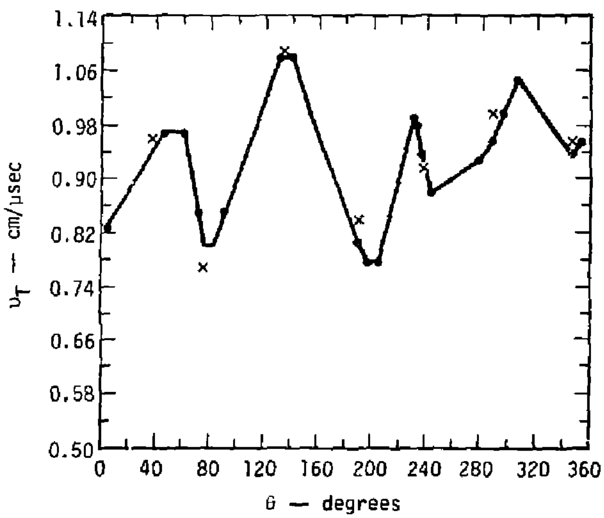
1.14
1.06
0.98
0.90
0.82
0.74
0.66
0.58
0.50
ν_T — cm/μsec
0
40
80
120
160
200
240
280
320
360
θ — degrees

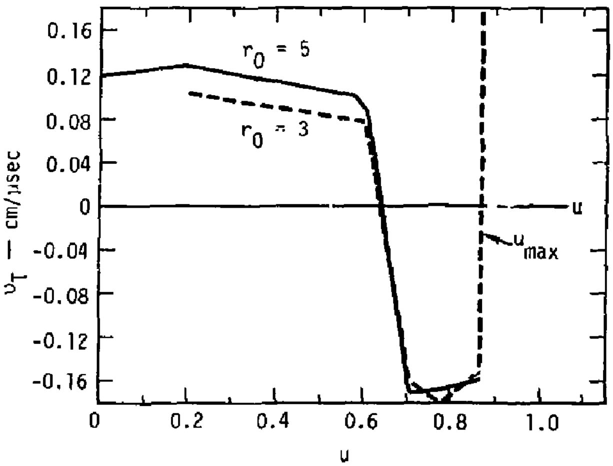
0.16
0.12
0.08
0.04
0
-0.04
-0.08
-0.12
-0.16
υ_T — cm/μsec
r_0 = 5
r_0 = 3
u
u_{max}
0
0.2
0.4
0.6
0.8
1.0
u